



Cite this: *Metallomics*, 2018, 10, 854

Systems impact of zinc chelation by the epipolythiodioxopiperazine dithiol gliotoxin in *Aspergillus fumigatus*: a new direction in natural product functionality†

Aliabbas A. Saleh,^a Gary W. Jones,^a Frances C. Tinley,^a Stephen F. Delaney,^a Sahar H. Alabbadi,^a Keith Fenlon,^a Sean Doyle^{a*} and Rebecca A. Owens^{a*}

The non-ribosomal peptide gliotoxin, which autoinduces its own biosynthesis, has potent anti-fungal activity, especially in the combined absence of the gliotoxin oxidoreductase GliT and bis-thiomethyltransferase GtmA. Dithiol gliotoxin (DTG) is a substrate for both of these enzymes. Herein we demonstrate that DTG chelates Zn^{2+} (m/z 424.94), rapidly chelates Zn^{2+} from $\text{Zn}(4\text{-(2-pyridylazo)-resorcinol})$ ($\text{Zn}(\text{PAR})_2$) and also inhibits a Zn^{2+} -dependent alkaline phosphatase (AP). Zn^{2+} addition rescues AP function following DTG-associated inhibition, and pre-incubation of DTG with Zn^{2+} completely protects AP activity. Zn^{2+} (1–50 μM) also significantly relieves the potent gliotoxin-mediated inhibition of *Aspergillus fumigatus* $\Delta\text{gliT}::\Delta\text{gtmA}$ ($p < 0.05$), which infers *in vivo* dithiol gliotoxin-mediated sequestration of free Zn^{2+} or chelation from intracellular metalloenzymes as inhibitory mechanisms. Quantitative proteomic analysis revealed that excess Zn^{2+} alters the effect of gliotoxin on *A. fumigatus* ΔgliT , with differential abundance of secondary metabolism-associated proteins in the combinatorial condition. GtmA abundance increased 18.8 fold upon co-addition of gliotoxin and Zn^{2+} compared to gliotoxin alone, possibly to compensate for disruption to GtmA activity, as seen in *in vitro* assays. Furthermore, DTG effected significant *in vitro* aggregation of a number of protein classes, including Zn^{2+} -dependent enzymes, while proteins were protected from aggregation by pre-incubating DTG with Zn^{2+} . We conclude that DTG can act *in vivo* as a Zn^{2+} chelator, which can significantly impede *A. fumigatus* growth in the absence of GliT and GtmA.

Received 9th March 2018,
Accepted 6th June 2018

DOI: 10.1039/c8mt00052b

rsc.li/metallomics

Significance to metallomics

Dithiol gliotoxin is a near-terminal biosynthetic intermediate from the gliotoxin biosynthetic pathway in the human pathogen *Aspergillus fumigatus*. Chemically reduced gliotoxin, dithiol gliotoxin (DTG), is revealed as a biological zinc chelator, and conversely, zinc can relieve the hitherto cryptic fungal autotoxicity of DTG. There is a systems-wide impact of zinc chelation by DTG on the fungal proteome, and we suggest it is DTG, as opposed to gliotoxin, which chelates zinc from metalloproteins. Since gliotoxin can be sequestered by both fungi and bacteria, our findings infer a new avenue to interfere with, and exploit, cellular zinc homeostasis in microorganisms.

Introduction

Gliotoxin and holomycin are microbial natural products, which are produced by fungal and bacterial spp., respectively (Fig. 1).^{1–3} Both are low molecular mass metabolites, and each contains a

disulphide bridge formed by the action of oxidoreductases, namely GliT and HlmI, on the respective dithiol precursor (Fig. 1).^{4–6} Disulphide bridge formation is essential for microbial self-protection against these reactive dithiol intermediates, and is a pre-requisite for the Major Facilitator Superfamily transporter GliA-mediated secretion of gliotoxin by *Aspergillus fumigatus*.^{5–8} Both metabolites are also present as bis-thiomethylated forms, and gliotoxin bis-thiomethyltransferase GtmA converts dithiol gliotoxin (DTG) to bis-dethiobis(methylthio)gliotoxin (BmGT) in *A. fumigatus*, whereas the origin of the cognate activity against dithiol holomycin in *Streptomyces clavuligeris* is unknown (Fig. 1).^{9,10} Bernardo *et al.* have shown that upon uptake by eukaryotic cells,

^a Department of Biology, Maynooth University, Co. Kildare, Ireland.
E-mail: sean.doyle@mu.ie, rebecca.owens@mu.ie; Tel: +353-1-708-3858, +353-1-708-3839

^b Centre for Biomedical Research, School of Clinical and Applied Sciences, Leeds-Beckett University, Leeds LS1 3HE, UK

† Electronic supplementary information (ESI) available. See DOI: 10.1039/c8mt00052b



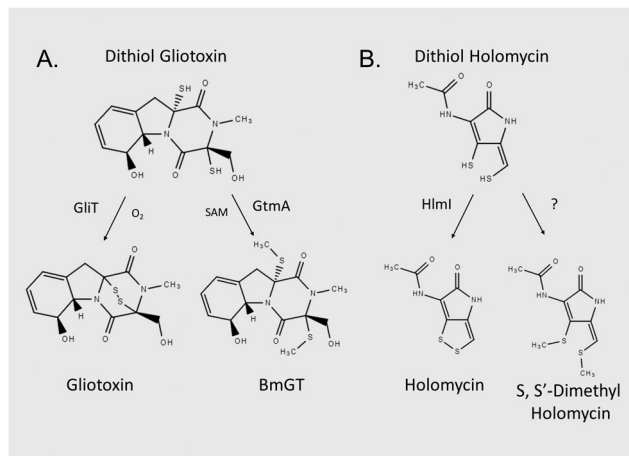


Fig. 1 Unrelated microbial dithiol-containing compounds undergo equivalent biotransformations, and appear to be co-substrates for two enzyme functionalities. (A) In *Aspergillus fumigatus*, DTG is either oxidised to gliotoxin via gliotoxin oxidoreductase GliT or bis-thiomethylated by gliotoxin bis-thiomethyltransferase GtmA. (B) In *Streptomyces clavuligeris*, dithiol holomycin undergoes oxidoreductase HmlI-mediated conversion to holomycin. The enzyme which catalyses S,S'-dimethyl holomycin formation remains to be identified.

gliotoxin is chemically reduced to the dithiol form by intracellular glutathione (GSH).¹¹ Carberry *et al.* revealed significantly elevated intracellular GSH in gliotoxin-sensitive *A. fumigatus* $\Delta gliT$ and that *Saccharomyces cerevisiae* $\Delta gsh1$, deficient in intracellular GSH, was resistant to exogenous gliotoxin.¹² The epipolythiodioxopiperazine (ETP) gliotoxin autoinduces its own biosynthesis by activating *gli* biosynthetic gene cluster expression, and BmGT formation has been shown to result in *gli* cluster attenuation in *A. fumigatus*, which results in the repression of gliotoxin biosynthesis.^{9,13,14} Methylation of dithiol holomycin has been proposed as a back-up plan for self-protection, and Dolan *et al.* revealed that *A. fumigatus* $\Delta gliT::\Delta gtmA$ is significantly more sensitive to exogenous gliotoxin than a *gliT*-deficient mutant.¹⁵ This suggests that the combined absence of both self-protection and negative regulation of DTG biosynthesis (or its intracellular presence) results in potent growth retardation – the precise cause of which is unknown.^{10,15}

Gliotoxin, other ETPs and dithiopyrrolones have been shown to inhibit the activity of many enzymes, and functionality of specific proteins.^{16–21} Several studies have demonstrated that the disulphide moiety of gliotoxin is responsible for most of the associated bioactivity of this molecule, whereas the S-methylated BmGT molecule is relatively inactive.^{17,22} In general, reactivity of gliotoxin towards protein thiols, damage from redox cycling, and Zn^{2+} ejection have been proposed as the respective mechanisms whereby protein functionality is altered. Interestingly, addition of the reducing agent, L-dithiothreitol (DTT), significantly augmented the inhibitory activity of gliotoxin towards farnesyltransferase, and either DTT or GSH augmented gliotoxin-mediated inhibition of equine alcohol dehydrogenase.^{16,17} Notably, neither of the aforementioned studies posited DTG-mediated Zn^{2+} chelation from either Zn^{2+} -dependent enzyme as the inhibitory mechanism.

In combination, these observations led us to hypothesise that, acting as a potent Zn^{2+} chelator, DTG (and not gliotoxin), could exhibit an equivalent mechanism of action towards Zn^{2+} -dependent enzyme systems. Moreover, DTG interference with Zn^{2+} availability or Zn^{2+} -dependent enzyme activity in *A. fumigatus* $\Delta gliT::\Delta gtmA$ could be the basis for observed and extreme growth retardation.¹⁵ However, it is also essential to consider a mechanistic reciprocity between DTG and Zn^{2+} . Consequently, while DTG may chelate the cation and impede Zn^{2+} -mediated enzyme activities, excess or available metal ion may provide protection against intracellular DTG. Indeed, zinc salts have been successfully used to reverse ovine and bovine facial eczema associated with exposure to fungal ETPs such as sporidesmin A, a related disulphide-containing metabolite secreted by *Pithomyces chartarum*.²³ It is postulated that Zn^{2+} chelates formed with sporidesmin A may attenuate its unwanted biological effects. Interestingly, Woodcock *et al.* presented mass spectrometric evidence of Zn^{2+} [sporidesmin] chelates, and noted that Zn^{2+} [gliotoxin] chelates, following $NaBH_4$ -mediated reduction, also existed, namely $[2\text{gliotoxin} + Zn]^{2-}$, $[2\text{gliotoxin} + Zn + Na]^-$ and $[\text{gliotoxin} + ZnCl]^-$ (m/z 427).²⁴ These authors speculated that that mono-ligands with halide coordination were the preferable complex form, however corresponding mass spectra and fragmentation patterns were not presented.

The ZafA transcriptional regulator, which can induce expression of the Zn^{2+} transporters *zrfA*, *zrfB* and *zrfC*, regulates zinc homeostasis in *A. fumigatus* and is essential for virulence.^{25–28} ZrfC is the key essential transporter which effects Zn^{2+} acquisition by *A. fumigatus*, while ZrfA and ZrfB play accessory and non-essential roles.²⁶ Interestingly, transporter ZrfB (AFUA_2G03860) was found to be significantly increased in abundance (\log_2 -fold increase: 1.31) in long-term *A. fumigatus* $\Delta gtmA$ cultures, which suggests interplay between dysregulated gliotoxin biosynthesis and Zn^{2+} homeostasis.²⁹

Herein, for the first time we reveal DTG as a Zn^{2+} chelator which can specifically and significantly inhibit Zn^{2+} -dependent metalloenzyme activity. Moreover, we demonstrate that Zn^{2+} significantly reverses the inhibitory effects of gliotoxin on *A. fumigatus* $\Delta gliT::\Delta gtmA$, which implicates intracellular Zn^{2+} chelation as a potential growth inhibitory strategy against this pathogen.¹⁵ Significant proteomic remodelling in *A. fumigatus* $\Delta gliT$ in response to gliotoxin versus Zn^{2+} /gliotoxin exposure further illuminates a hitherto unanticipated *in vivo* interaction between DTG and Zn^{2+} .

Methods

High resolution mass spectrometry detection of gliotoxin complexed to Zn^{2+}

Tris(2-carboxyethyl)phosphine hydrochloride (TCEP)-reduced gliotoxin (DTG; 300 μM final) was mixed with $ZnSO_4 \cdot 7H_2O$ in the presence of formic acid (0.1% (v/v)) to achieve 0.5, 1 and 3-fold molar equivalents of Zn^{2+} to DTG. Samples were passed through 0.22 μm spin filters and directly injected onto a Thermo Q-Exactive Mass spectrometer (5 μl min⁻¹). Assessment of DTG- Zn^{2+}



complex formation was evaluated by both positive and negative ESI mode with full MS scan (50–2000.00). The following settings were used in the analysis: spray voltage (negative mode: 3.6 kV, positive mode 4 kV), capillary temperature 320 °C.

Assessment of *in vitro* Zn²⁺ chelation by DTG

Zinc binding assays were performed as described in Chan *et al.* with some modifications.³⁰ Titrations were carried out in PBS pH 7.4 (1 ml final volume). 4-(2-Pyridylazo)-resorcinol (PAR) (80 µl; 1.5 mM) was added with 60 µl 1 mM ZnSO₄, per ml to yield final ratio of 2 : 1 (PAR : Zn²⁺). DTG (2.5 mM in methanol) was prepared by 60 min pre-incubation with 12.5 mM TCEP in 100 µl final volume and was then added in increasing concentration to yield 1, 2, 3, 4 and 5 molar equivalents of DTG to Zn(PAR)₂ (final concentrations: 60 µM Zn²⁺, 120 µM PAR, 60–300 µM DTG). 12.5 mM TCEP in methanol and oxidised gliotoxin (2.5 mM) were used as negative controls. After addition of all components, absorbance spectra were recorded between 200–800 nm.

Alkaline phosphatase (AP) and GtmA enzyme assays

Zn²⁺-Dependent AP from bovine intestinal mucosa (AP; 1.44 U ml⁻¹ (Sigma-Aldrich)) in PBS was pre-incubated with the following agents to determine the extent of enzyme inhibition: 5 mM EDTA, 150 µM gliotoxin (GT), 10–150 µM DTG (TCEP-reduced GT), 50 µM TPEN (*N,N,N',N'*-tetrakis(2-pyridylmethyl)ethane-1,2-diamine), 50 µM–5 mM DTT, or 50 µM–5 mM GSH for 15 min in triplicate. Control or treated AP (50 µl per reaction) was added to 1 ml *p*-nitrophenol phosphate (pNPP) (5 mM; dissolved in PBS with 50 mM glycine pH 9.5) and assayed in triplicate at 37 °C for 30 min. Enzyme reactions were terminated by addition of 20 mM NaOH (5 ml). AP activity was determined by *p*-nitrophenol (pNP) detection at 405 nm following pNPP hydrolysis. The protective effect of pre-incubating DTG or TPEN with Zn²⁺ was also evaluated using this assay system. DTG (50 µM) or TPEN (50 µM) were pre-incubated with Zn²⁺ (25–100 µM) for 15 min prior to addition of AP enzyme and the rest of the assay was performed as before. To test the capacity of Zn²⁺ to rescue DTP-associated loss of AP activity, AP was pre-incubated with DTG (50 µM) for 15 min, followed by addition of Zn²⁺ (0.1–1 mM) for a further 15 min, prior to addition of pNPP substrate.

GtmA activity was determined as described in Dolan *et al.* to evaluate the effect of Zn²⁺ (molar ratio 0.0001–10 Zn²⁺ : 1 DTG) on the formation of BmGT.¹⁵ Briefly, *S*-adenosylmethionine (SAM) (1 µM final) and TCEP-reduced gliotoxin (250 µM final) were combined, along with PBS. Zn²⁺ was added at a range of concentrations (0.025, 0.25, 2.5, 25, 125, 250 µM and 2.5 mM), representing a molar ratio ranging from 0.0001 to 10 : 1 Zn²⁺ : DTG. A control was also prepared with no Zn²⁺ added. GtmA (0.5 µM) was added to the mixture followed by incubation at 37 °C for 5 min. Reactions were stopped by protein precipitation using TCA (final 15%) and incubation on ice for 20 min. Clarified mixtures were analysed by RP-HPLC and absorbance monitored at 254 nm to determine the concentration of BmGT and monomethyl gliotoxin (MmGT).

Assessment of the effect of Zn²⁺ on alkylation of DTG

Iodoacetamide (IAA) was used as an alkylating agent to investigate the effect of Zn²⁺ on alkylation of DTG. IAA stock (50 mM) was prepared in 50 mM ammonium bicarbonate. 3 mM DTG was prepared by 60 min pre-incubation of gliotoxin with 12.5 mM TCEP. DTG (0.3 mM final) was mixed with ZnSO₄ at a range of concentrations (0.1, 0.15, 0.3, 0.6, 0.9 mM) to achieve molar equivalents of Zn²⁺ to DTG of 0.33, 0.5, 1, 2 and 3, respectively. IAA was subsequently added at a final concentration of 3 mM (ratio IAA : DTG 10 : 1) and incubated in the dark for 20 min. All reactions were carried out in methanol at 100 µl final volume. Control samples were included to measure levels of DTG and alkylated gliotoxin formed in the absence of Zn²⁺. Reactions were evaluated by RP-HPLC.¹⁵

A. *fumigatus* phenotypic assays

A. fumigatus Δ*gliT* and Δ*gliT*::Δ*gtmA* strains were grown on MEA agar for 5 days at 37 °C. After incubation, conidia were harvested with PBST and washed three times with PBS and resuspended in PBS. Conidia were counted using haemocytometer and stored at 4 °C for future use. Conidia were serially diluted to 10³ µl⁻¹ and 5 µl was spotted on Czapek-Dox agar plates (permissive for endogenous gliotoxin biosynthesis⁷) containing gliotoxin (0, 15 or 30 µM) and Zn²⁺, respectively. Plates were then incubated at 37 °C and growth monitored up to 96 h by measuring radial growth (mm) of each colony. Two-way ANOVA analysis was performed to determine the statistical significance between strains at different concentrations of gliotoxin and Zn²⁺.

Extraction and measurement of extracellular and intracellular gliotoxin

A. fumigatus wild-type and Δ*gliT*::Δ*gtmA* were grown in Sabouraud-dextrose media for 21 h and gliotoxin was subsequently added for 3 h at 15 µM with and without Zn²⁺ (*n* = 3 biological replicates for all specimens). Zn²⁺ was added at 1 mM final concentration. Supernatant samples were taken after 15, 30, 60, 120 and 180 min and were extracted using chloroform (1 : 1), as described.³¹ The organic extracts were subsequently dried down and resuspended in methanol and analysed for gliotoxin content using RP-HPLC with UV detection (Shimadzu), using polar C18 RP-HPLC column (Phenomenex polar C18 Luna Omega column (150 mm × 4.6 mm, 5 µm)) at a flow rate of 1 ml min⁻¹. A mobile phase of acetonitrile and water with 0.1% (v/v) TFA was used under gradient conditions. *A. fumigatus* wild-type was also grown in Czapek-Dox media for 72 h (gliotoxin-producing conditions) in the presence of either low (0.027 mM) or high (0.5 mM) Zn²⁺ (*n* = 3 biological replicates for all specimens). Controls were included, with no Zn²⁺ added. Aliquots were taken every 24 h and organic extractions and RP-HPLC analyses were performed as outlined above. For intracellular gliotoxin recovery, mycelia collected after 3 h incubation were harvested and snap frozen in liquid N₂. Intracellular gliotoxin was extracted as described previously for SAM, using a modified protocol.⁸ Briefly, mycelia were ground using liquid N₂ with a mortar and pestle. 100 mg mycelia were incubated with 0.1 N HCl (250 µl) on ice for 1 h



with intermittent vortexing. Protein was removed by addition of 100% TCA to achieve a final concentration of 15% (v/v) TCA. After centrifugation at $16\,000 \times g$, supernatants were collected and then analysed by RP-HPLC.

Proteomic analysis of gliotoxin affects, with and without Zn^{2+} , on *A. fumigatus* ΔgliT

A. fumigatus ΔgliT was cultured ($n = 3/\text{condition}$) for 21 h in Sabouraud-dextrose media (SDM) followed by addition of gliotoxin (15 μM) or methanol (control) with and without ZnSO_4 (1 mM) addition for 3 h. Mycelia were then harvested and snap frozen in liquid N_2 . Mycelia were lysed using buffer (100 mM Tris-HCl, 50 mM NaCl, 20 mM EDTA, 10% v/v glycerol, 1 mM PMSF, 1 $\mu\text{g ml}^{-1}$ pepstatin A, pH 7.5) with grinding and sonication, and clarified using centrifugation.⁸ The protein lysates were then subjected to precipitation using TCA/acetone and resuspended in 100 mM Tris-HCl, 6 M urea, 2 M thiourea, pH 8.0. Samples were then reduced by DTT and followed by alkylation using IAA. This was followed by addition of sequencing grade trypsin combined with Protease Max surfactant for overnight digestion. Following sample clean-up using Millipore C18 ZipTips, all peptide mixtures were analysed *via* a Thermo-Fisher Q-Exactive mass spectrometer coupled to a Dionex RSLCnano.³² LC gradients ran from 4% to 35% ACN over 2 h, and data were collected using a Top15 method for MS/MS scans. Comparative proteome abundance and data analysis was performed using MaxQuant software (v. 1.5.3.30), with PERSEUS used to organize data (v. 1.5.4.0).^{33,34} Proteins with significant changes in abundance ($p < 0.05$; fold change ≥ 2) signified quantitative changes between the sample treatments. Qualitative differences were also noted, where proteins were not detected in one group and were present in at least 2 replicates from the comparator group. Functional analysis was carried out using FungiFun2 (<https://elbe.hki-jena.de/fungifun/fungifun.php>).³⁵

In vitro DTG induced-protein aggregation assays

Protein extracts were prepared from *A. fumigatus* mycelia from three biological replicates, previously cultured in SDM at 37 °C, for 24 h at 200 rpm. Mycelia were harvested by filtering through Miracloth, snap-frozen and ground in liquid N_2 using a pestle and mortar. Lysis buffer (0.1 M Tris-HCl, 50 mM NaCl, 1 mM PMSF pH 7.5; 400 μl) was added to ground mycelia (200 mg) and lysed by sonication. Lysates were clarified by centrifugation at $12\,000g$, 4 °C for 10 min and this was repeated twice to remove insoluble material. Lysates were diluted to 1 mg ml^{-1} and subjected to the following treatments in triplicate: (a) control: methanol and TCEP were added as a solvent control; (b) DTG: TCEP-reduced gliotoxin was added to the protein extracts to a final concentration of 150 μM and (c) DTG/ Zn^{2+} :TCEP-reduced gliotoxin was pre-mixed with $\text{ZnSO}_4 \cdot 7\text{H}_2\text{O}$ at a 1 : 3 molar ratio. The mixture was added to the protein extracts in triplicate to achieve a final concentration of 150 μM DTG and 450 μM Zn^{2+} . All samples were incubated at 50 °C for 30 min prior to addition of solubilisation buffer and analysis by SDS-PAGE. Protein aggregates were observed as a band of Coomassie-stained protein at the interface between the stacking and resolving

gels. These bands were excised and subjected to in-gel digestion according to Shevchenko *et al.*³⁶ Peptide mixtures were de-salted using C₁₈ Zip-tips and analysed using Label-free quantitative proteomics (Thermo Q-Exactive LC-MS). Data analysis was performed using MaxQuant with Perseus for data organisation and statistical analysis.^{9,32}

Results

DTG chelates Zn^{2+} *in vitro*

High resolution mass spectrometry, spectrophotometry, and chemical and enzyme assays were used to investigate the formation of a complex between DTG and Zn^{2+} . Following TCEP-mediated reduction of gliotoxin and Zn^{2+} addition, negative mode MS analysis revealed the presence of a $\text{Zn}[\text{dithiolate gliotoxin}]$ complex with $m/z = 424.93851$, corresponding to a Cl^- adduct of the metal chelate (Fig. 2A and Fig. S1, ESI†). Furthermore, DTG also competitively dissociated Zn^{2+} from a $\text{Zn}[(4-(2\text{-pyridylazo})\text{-resorcinol})_2]$ $\text{Zn}(\text{PAR})_2$ complex, whereby DTG (60–300 μM) addition resulted in a corresponding decrease in $A_{493\text{nm}}$ of $\text{Zn}(\text{PAR})_2$, corresponding to Zn^{2+} chelation (Fig. 2B). Relevantly, gliotoxin had no effect on $\text{Zn}(\text{PAR})_2$ interaction which confirmed the specific role of the dithiol moiety of reduced gliotoxin in chelation (Fig. S2, ESI†). To investigate the effect of Zn^{2+} on the enzymatic *S*-methylation of DTG, a GtmA activity assay was performed. GtmA bis-thiomethylates DTG to form BmGT using SAM as the methyl source (Fig. 1).⁹ Gliotoxin *S*-methylation occurs in a sequential manner, with mono-methylated species (MmGT) appearing initially, followed by formation of BmGT.^{9,15,37} Zn^{2+} inhibits GtmA-mediated thio-methylation of gliotoxin *in vitro* in a concentration-dependent manner, most likely due to an inability to recognise and bind $\text{Zn}^{2+}[\text{DTG}]$ (Fig. 2C). Support for DTG thiol protection by Zn^{2+} coordination was provided by an alkylation assay. Although IAA modifies DTG to alkylated gliotoxin, Zn^{2+} also inhibits alkylation of DTG which further strengthens the concept of thiol occlusion *via* Zn^{2+} chelation (Fig. 2D and Fig. S3, ESI†).

DTG inhibits AP by Zn^{2+} chelation

To investigate the ability of DTG to inhibit the activity of a zinc-dependent metalloenzyme, AP activity assays were carried out. Gliotoxin was reduced to DTG as described above and confirmed by RP-HPLC (data not shown). DTG inhibited AP in a dose-dependent manner (0–150 μM DTG) and time-dependent manner (Fig. 3A and Fig. S4, ESI†). Solvent controls (containing TCEP and methanol) did not show any significant AP inhibition. While 50 μM DTG significantly inhibited AP activity ($p < 0.001$), pre-incubation of DTG (50 μM) with Zn^{2+} (25 μM –1 mM) alleviated DTG-associated AP inhibition (Fig. 3B). The Zn^{2+} chelator TPEN was also tested, but only produced a minor decrease in AP activity (11%) when used at the same concentration as DTG (50 μM) (Fig. 3C). EDTA (5 mM), a metal ion chelator, inhibited AP activity by approx. 30–40% (Fig. S5, ESI†). AP activity was not significantly inhibited by 150 μM GT, 50 μM –5 mM of the cellular reductant GSH or 50 μM –1 mM of the thiol-containing reductant DTT (Fig. S5, ESI†). Lack of inhibition by GT, TCEP, GSH or DTT



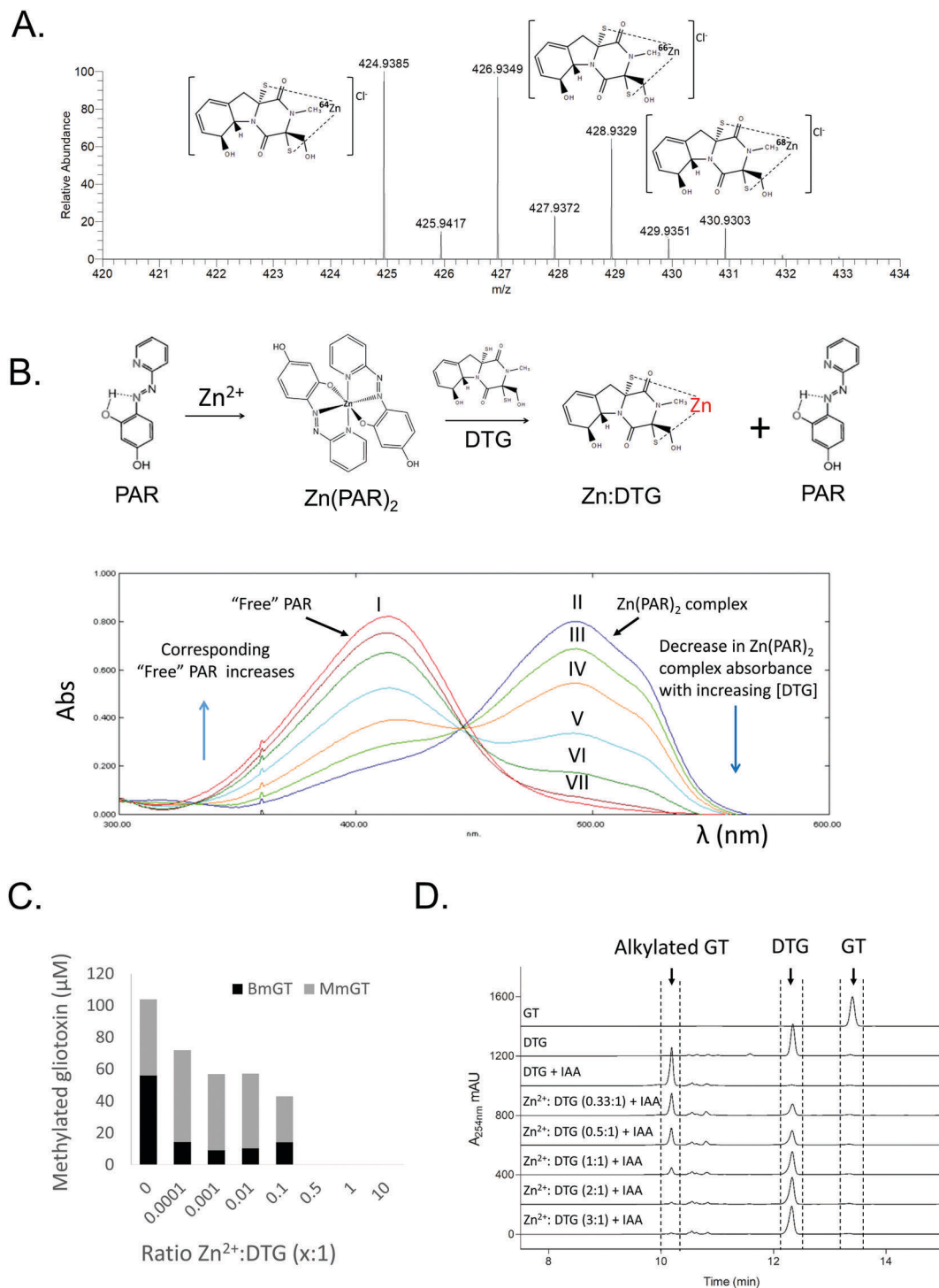


Fig. 2 Characterisation of DTG as a Zn^{2+} chelator. (A) Dithiolate gliotoxin complexed with Zn^{2+} (Cl^- adduct) with accompanying isotopic analysis in negative ion mode MS (direct injection). Structure of DTG:Zn complex is depicted with positioning of the metal ion between the two thiolates, although exact coordination with other groups is unknown. (B) DTG chelates Zn^{2+} from Zn(PAR)_2 (Zn(PAR)_2 $\text{pK}_a = 12.15$)⁴⁴ in a concentration-dependent manner. Overlaid UV-vis profiles of PAR alone (I; red), and Zn(PAR)_2 (II; blue). DTG added in increased concentration to Zn(PAR)_2 1–5 molar equivalents of oxidised gliotoxin to Zn^{2+} ; III–VII, respectively. Decrease in $A_{493\text{nm}}$ is accompanied by increase in $A_{413\text{nm}}$ as free PAR is released. (C) Zn^{2+} inhibits GtmA-mediated methylation of DTG in a concentration dependent manner. Zn^{2+} was included in the methylation assay at a molar ratio ranging from 0.0001 to 10 : 1 (DTG). A control containing no Zn^{2+} was included. Concentration (μM) of BmGT and MmGT formed after 5 min was determined by RP-HPLC. (D) Zn^{2+} inhibits IAA-mediated alkylation of DTG in a concentration-dependent manner. RP-HPLC analysis (detection at 254 nm) reveals the inhibitory effect of Zn^{2+} on DTG alkylation.

strongly infers that inhibition is not caused by AP disulphide bridge cleavage or thiol modification. Zinc addition for 30 min reverses DTG-induced inhibition of AP, which further implicates Zn^{2+} chelation as the mechanism of inhibition (Fig. S6, ESI†).



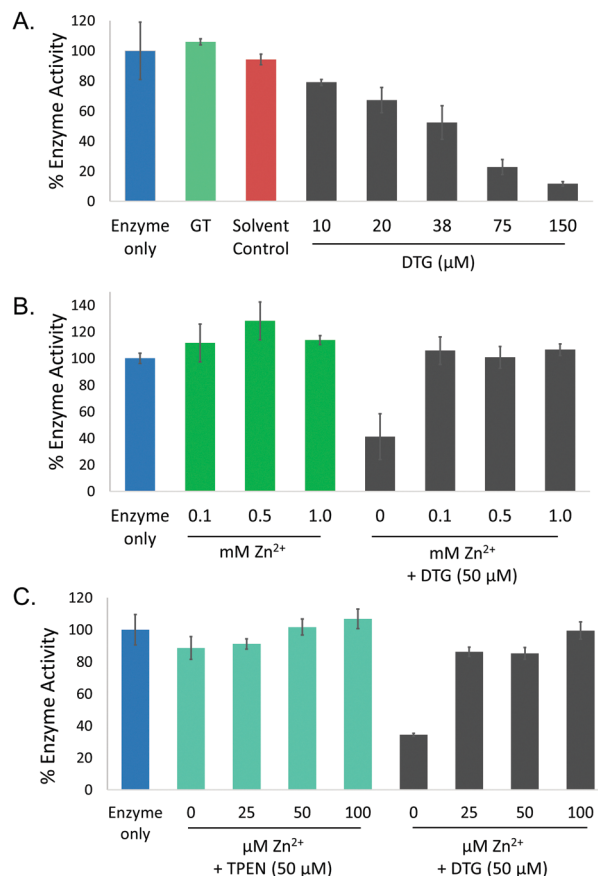


Fig. 3 DTG inhibits AP activity by Zn²⁺ chelation. (A) Dose-dependent (10–150 μM DTG) inhibition of AP activity, with IC₅₀ = 38 μM DTG. Neither GT or the solvent control (12.5 mM TCEP in methanol) inhibit AP activity. (B) Pre-incubation of DTG with Zn²⁺ (0.1, 0.5 and 1 mM) prevents DTG-mediated enzyme inhibition. (C) TPEN (50 μM) has no significant impact on AP activity (89% activity compared to control). Pre-incubation of DTG with Zn²⁺ (25–50 μM) significantly recovered AP activity to 86% of the control.

Impact of Zn²⁺ exposure on *A. fumigatus* Δ gliT and Δ gliT:: Δ gtmA, in the presence of exogenous gliotoxin

In order to determine whether Zn²⁺ had an impact on gliotoxin-associated growth inhibition, plate assays were carried out using *A. fumigatus* strains deficient in enzymes that use DTG as their substrate, Δ gliT:: Δ gtmA and Δ gliT. Severe radial growth inhibition of *A. fumigatus* Δ gliT:: Δ gtmA in the presence of gliotoxin (15 μM)¹⁵ (Fig. 4A) was significantly relieved ($p < 0.005$) in the presence of 1–10 μM Zn²⁺, and relief of gliotoxin-mediated growth inhibition was maintained up to 50 μM Zn²⁺. Radial growth of *A. fumigatus* Δ gliT:: Δ gtmA was unaffected by Zn²⁺ (1–50 μM). Higher concentrations of Zn²⁺ significantly inhibited the growth of both *A. fumigatus* Δ gliT:: Δ gtmA (100 μM–1 mM; Fig. 4) and *A. fumigatus* Δ gliT (1–2 mM; Fig. S7, ESI[†]). This correlates with a decrease in the rescue effect of Zn²⁺ on gliotoxin-associated growth inhibition in *A. fumigatus* Δ gliT:: Δ gtmA. The combination of gliotoxin (15–30 μM) and excess Zn²⁺ (1–2 mM) produced further inhibition of radial growth of *A. fumigatus* Δ gliT at 96 h ($p < 0.005$) compared to the growth reduction observed in either the presence of Zn²⁺ or gliotoxin alone (Fig. S7, ESI[†]).

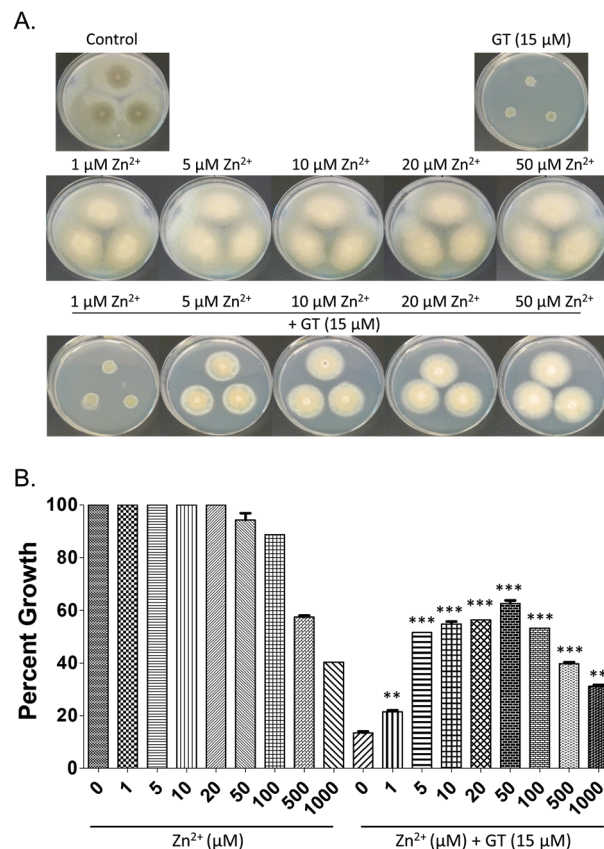


Fig. 4 (A) Potent growth inhibitory effect of gliotoxin (15 μM) on *A. fumigatus* Δ gliT:: Δ gtmA is significantly ($p < 0.005$) reversed by co-addition of Zn²⁺ (1–50 μM). Zn²⁺ (0–50 μM) has a negligible effect on mutant growth. (B) Graphical representation of same in terms of relative growth percentages. Note that higher Zn²⁺ levels (100 μM–1 mM) result in dissipation of the relief, in line with Zn²⁺-associated toxicity noted in controls.

Zn²⁺ augments gliotoxin uptake and efflux in *A. fumigatus* wild-type and Δ gliT:: Δ gtmA

Previous studies have revealed that exogenous gliotoxin is sequestered by *A. fumigatus*.³⁸ To further explore the interaction between Zn²⁺ and gliotoxin *in vivo*, both *A. fumigatus* wild-type and Δ gliT:: Δ gtmA were exposed to gliotoxin (15 μM) for 3 h in the presence and absence of Zn²⁺ (1 mM). In all conditions uptake of gliotoxin by *A. fumigatus* was evident by decreasing levels detected in culture supernatants across the incubation times, and corresponding increases in intracellular gliotoxin concentration (Fig. S8, ESI[†]). Fig. S8A–D (ESI[†]) show that excess Zn²⁺ augmented gliotoxin uptake in both *A. fumigatus* wild-type and Δ gliT:: Δ gtmA. In the presence of Zn²⁺ (1 mM), with significantly less gliotoxin detected in *A. fumigatus* wild-type culture supernatants 30 min after addition (Fig. S8A–C; $p < 0.05$, ESI[†]). Zn²⁺ effected a more marked response in *A. fumigatus* Δ gliT:: Δ gtmA, with a significant decrease in extracellular gliotoxin levels at every time point (15–180 min; Fig. S8B; $p < 0.05$, ESI[†]). When excess Zn²⁺ was present in the culture medium, initial rates of gliotoxin uptake increased from 38.32 ± 5 to 55.04 ± 8.78 ng min^{−1} ml^{−1} of culture (mean \pm SEM) in *A. fumigatus* wild-type and from 5.06 ± 7.16 to 75.94 ± 7.38 ng min^{−1} ml^{−1} of culture (mean \pm SEM)



in $\Delta gliT::\Delta gtmA$. Commensurate increases in intracellular gliotoxin (ng/100 mg mycelia) were observed in both *A. fumigatus* wild-type and $\Delta gliT::\Delta gtmA$, in the presence of Zn^{2+} (Fig. S8D, ESI†). Intracellular levels of gliotoxin were significantly increased in *A. fumigatus* wild-type upon Zn^{2+} co-addition ($p < 0.01$), likely due to inhibition of GtmA-catalysed BmGT formation and efflux. Elevated intracellular gliotoxin levels in $\Delta gliT::\Delta gtmA$ correlated with an increased rate of gliotoxin uptake induced by Zn^{2+} (Fig. S8, ESI†). Intracellular DTG was not detectable due to either spontaneous intracellular or extraction-associated oxidation.

LFQ proteomic analysis reveals that Zn^{2+} alters the effect of gliotoxin on *A. fumigatus* $\Delta gliT$

To further investigate the nature of the combinatorial inhibition of *A. fumigatus* $\Delta gliT$ during simultaneous exposure to Zn^{2+} and gliotoxin, compared to gliotoxin alone, comparative LFQ proteomic analysis was carried out. Overall, 47 proteins exhibited unique presence and 23 proteins were significantly increased in abundance in *A. fumigatus* $\Delta gliT$ upon combinatorial exposure (Zn^{2+}/GT) compared to gliotoxin only (Table S1, ESI†). Conversely, 45 proteins were absent and 10 proteins showed significantly reduced abundance in *A. fumigatus* $\Delta gliT$ upon combinatorial exposure compared to gliotoxin only (Table S1, ESI†). Functional analysis revealed that zinc-ion binding proteins were significantly enriched (8/70 proteins; $p = 0.005$) among proteins with elevated abundance or uniquely detected in the presence of Zn^{2+}/GT compared to gliotoxin alone (Table 1 and Fig. S9, ESI†). Notably, secondary metabolism-associated proteins were altered in abundance, or demonstrated qualitative changes in the combined condition (Zn^{2+}/GT) compared to gliotoxin only (Table 2). These included the ferrirococin synthetase SidC, which was repressed by gliotoxin, but not by the combined condition, as were four members of the fumagillin biosynthetic cluster (Table 2 and Table S1, ESI†). Consequently, when *A. fumigatus* was grown in gliotoxin-producing conditions, Zn^{2+} caused a significant increase in fumagillin levels even at lower levels (0.027 mM Zn^{2+} ; $p < 0.001$) (Fig. S10, ESI†).

Low affinity zinc transporter ZrfB, which is ZafA-dependent and normally induced by zinc depletion, was undetectable in the combinatorial exposure condition, which suggests a zinc-limiting environment in gliotoxin-only exposure (Table 1). Likewise, allergen AspF2 which is expressed under zinc-limiting conditions, and shares a divergent promoter with *zrfC*, was absent upon co-exposure.³⁹ It was also observed that GliM, a component of the gliotoxin biosynthetic capacity was absent, which infers that gliotoxin biosynthesis may be attenuated in the combinatorial exposure scenario (Table 2). Indeed, Zn^{2+} presence completely abrogated gliotoxin biosynthesis in Czapek-Dox media (Fig. S10, ESI†). These observations pertaining to impeded gliotoxin biosynthesis are further supported by the absence of GpgA (AFUA_1G05210), a G-protein coupled receptor subunit, previously shown to be essential for gliotoxin production in *A. fumigatus*.⁴⁰ It is also notable that the nonribosomal peptide synthetase NRPS8/Pes3⁴¹ (AFUA_5G12730) was absent following co-exposure to Zn^{2+} and gliotoxin, which suggests that it may contribute to adaptation to zinc-limiting conditions.

Gliotoxin exposure induces elevated GtmA abundance in *A. fumigatus* $\Delta gliT$,⁹ and Manzanares-Miralles *et al.* reported that gliotoxin induces significantly increased abundance of the GtmA ortholog in *Aspergillus niger*, in which the *gli* cluster is absent.³⁷ Interestingly, while Zn^{2+} exposure alone had no significant effect on the abundance of GtmA in *A. fumigatus*, combinatorial exposure with gliotoxin resulted in significantly elevated GtmA abundance (18.8-fold and $p < 0.01$) compared to that in the presence of gliotoxin only (Table 2). Allied to GtmA activity data (Fig. 2C), this suggests that *in vivo* chelation of Zn^{2+} by DTG may prevent substrate access to GtmA, thereby resulting in a further increased abundance of the enzyme (Fig. 5A).

Manifestation of heat-induced *in vitro* protein aggregation in *A. fumigatus* mycelial lysates, specifically by DTG

Inhibition of Zn^{2+} -dependent enzyme activities, combined with the observed *in vivo* interplay between the divalent metal cation

Table 1 Zinc associated proteins with differential abundance, or uniquely detected, between the combination condition (Zn^{2+}/GT) and the gliotoxin – only control

Protein description	Log ₂ fold change ^a (<i>p</i> value)	Uniquely detected ^b	Peptides	Gene IDs (AFUA_)
Zinc ion binding				
Zinc knuckle domain protein (Byr3), putative	−1.33 (0.021)	Zn^{2+}/GT	9	1G07630
Rho GTPase activator activity Rga	N/A		4	1G12680
Putative zinc-binding dehydrogenase family oxidoreductase	1.55 (0.0018)		16	1G15610
Putative formaldehyde dehydrogenase	1.54 (0.0027)		15	2G01040
Putative carbonic anhydrase CafA	1.65 (0.0029)	Zn^{2+}/GT	12	4G11250
C-x8-C-x5-C-x3-H type zinc finger	N/A		5	4G13910
Putative zinc-dependent alcohol dehydrogenase AlcC	1.62 (0.0004)		30	5G06240
Cytidine deaminase, zinc ion binding activity	N/A		2	7G01040
Zinc knuckle nucleic acid binding protein, putative	N/A	Zn^{2+}/GT	2	7G02190
Putative carbonate dehydratase, zinc ion binding activity	1.67 (0.0041)	GT	7	8G06554
Zinc homeostasis				
Low affinity plasma membrane zinc transporter ZrfB	N/A	GT	3	2G03860
Allergen AspF2 AspF2	N/A	GT	7	4G09580

^a Negative values indicate protein was decreased in abundance in combination treatment (Zn^{2+}/GT) compared to the gliotoxin only treatment, while positive values indicate an increase in abundance. ^b Uniquely detected: protein uniquely identified in at least 2 biological replicates of either gliotoxin-only treated cultures or the combination condition (Zn^{2+}/GT).



Table 2 Secondary metabolism-related proteins with differential abundance, or uniquely detected, between the combination condition (Zn^{2+} /GT) and the gliotoxin-only control

Secondary metabolite	Protein description	\log_2 fold increase (<i>p</i> value)	Uniquely detected ^a	Peptides	Gene IDs (AFUA_)
Gliotoxin	Unknown function protein GliH	4.2361 (0.0052)	GT	3	6G09745
	O-Methyltransferase GliM		GT	4	6G09680
	Gliotoxin thiomethyltransferase GtmA			18	2G11120
NRPS8 (unknown)	NRPS8/Pes3		GT	3	5G12730
Ferricrocin	NRPS involved in ferricrocin siderophore biosynthesis SidC		Zn^{2+} /GT	5	1G17200
Fumagillin	Putative alpha/beta hydrolase FmaC		Zn^{2+} /GT	11	8G00380
	Unknown function protein FmaD		Zn^{2+} /GT	5	8G00400
	Protein encoded in the fumagillin gene cluster		Zn^{2+} /GT	10	8G00430
	Putative iron-dependent oxygenase FmaF		Zn^{2+} /GT	9	8G00480

^a Uniquely detected: protein uniquely identified in at least 2 biological replicates of either gliotoxin-only treated cultures or the combination condition (Zn^{2+} /GT).

and DTG in *A. fumigatus*, led us to further investigate the interaction between DTG and *A. fumigatus* proteins. DTG-associated protein destabilisation was investigated by exposing complex lysates to either DTG or a mixture of Zn^{2+} and DTG, followed by heat treatment. Exposure of *A. fumigatus* mycelial protein lysates to TCEP/methanol, DTG or a mixture of Zn^{2+} and DTG followed by SDS-PAGE analysis revealed near-identical electrophoretic patterns in the resolving gel (Fig. 5B). However, uniquely, following protein lysate exposure to DTG, and subsequent heat treatment (50 °C/30 min), either protein aggregation or an inability to

disaggregate unfolded proteins was observed (Fig. 5B). Mass spectrometry-based analysis of the proteins retained at the interface between the stacking and resolving gel identified 551 proteins in total from the three conditions tested. Label-free proteomics revealed 94 proteins uniquely detected or significantly elevated in the aggregates following DTG pre-treatment, relative to the control (Fig. 5C and Table S2, ESI[†]). DTG addition to *A. fumigatus* lysates elicits an overall increase in aggregated proteins compared to the controls. Functional analysis revealed a significant number of proteins with oxidoreductase activity ($n = 27$, $p = 0.019$), metal ion binding ($n = 16$, $p = 0.024$) and zinc ion binding ($n = 7$, $p = 0.047$) showed increased aggregation in response to DTG treatment (Fig. 5D). Notably, pre-incubation of DTG with Zn^{2+} prevented this aggregation in the case of 77% of the DTG-responsive proteins (72/94 proteins), whereby the combinatorial condition lead to significantly lower levels of protein aggregation compared to DTG treatment ($p < 0.05$). Additional stabilisation was observed in the combinatorial condition, as 77 proteins showed lower abundance in the aggregates compared to the control condition (Fig. 5C). Excess Zn^{2+} used in the pre-mixed DTG/ Zn^{2+} treatment could contribute to this additional stabilising effect.

Among the proteins affected by DTG-induced aggregation, was the zinc-dependent alcohol dehydrogenase AlcC, which was only detected in aggregates from lysates pre-incubated with DTG, indicating co-addition of Zn^{2+} prevented DTG-induced aggregation of this protein. Another protein detected exclusively in aggregates induced by DTG was the putative farnesyltransferase beta subunit Ram1 (AFUA_4G10330) which contains a C-terminal Zn^{2+} binding pocket, within the active site.^{42,43} A number metallo-peptidases were also increased or uniquely detected in DTG-induced aggregates (AFUA_6G09190, AFUA_4G07910, MepB), as well as the zinc-dependent methionine synthase MethI/D, while co-addition of Zn^{2+} generated aggregation profiles in line with the control.

Overall, these data suggest that DTG may chelate Zn^{2+} from selected cellular proteins thereby inducing protein unfolding and consequently resulting in temperature-induced aggregation. It is also possible that DTG inhibits selected components of the proteasome-mediated recognition and/or digestion of protein aggregates; which results in their persistence in DTG-treated

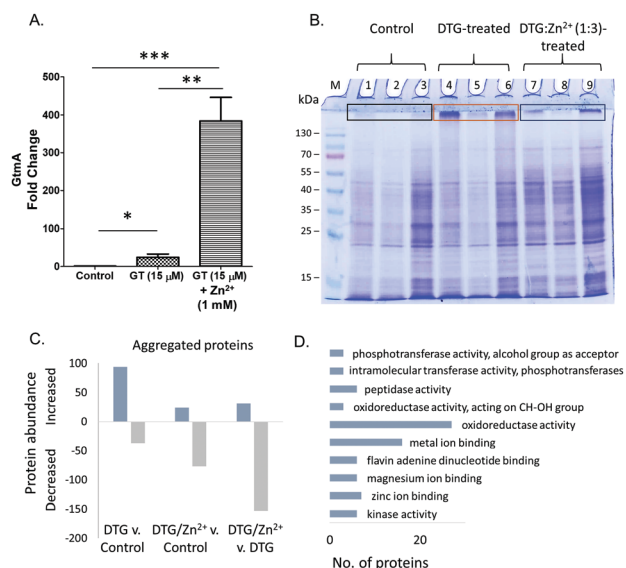


Fig. 5 (A) Fold change in GtmA abundance following gliotoxin (GT: 15 μM) and gliotoxin & Zn^{2+} (15 μM & 1 mM, respectively) exposure compared to controls in *A. fumigatus* Δ*gliT*. (B) SDS-PAGE analysis of 3 independently prepared *A. fumigatus* protein lysates. Lanes 1–3: negative controls: protein lysates treated with TCEP/methanol only. Lanes 4–6: protein lysates treated with DTG. Lanes 7–9: protein lysates treated with DTG: Zn^{2+} (1 : 3). M, molecular mass marker. Protein aggregation is evident (boxes) following DTG-exposure. (C) Number of proteins with increased or decreased abundance (qualitative and quantitative) in aggregates recovered from control, DTG or combined DTG/ Zn^{2+} treatments. (D) Functional analysis (FungiFun2) showing GO molecular function categories significantly enriched ($p < 0.05$) among proteins with increased abundance in DTG-induced aggregates. Arranged in order of ascending p value.



lysates. Finally, it is likely that some proteins detected in the aggregates may be present as a result of non-specific physical entrapment, however, these putative, non-specifically aggregated proteins are resistant to the dissolution effects of SDS solubilisation buffer and heat (95 °C/4 min).

Discussion

Herein, we provide evidence that DTG is a Zn^{2+} -chelator. We also reveal Zn^{2+} -metalloenzyme inhibition specifically by DTG, and not by gliotoxin or other reducing agents (DTT or GSH). This suggests Zn^{2+} chelation, as well as disulphide bridge cleavage or thiol modification, as a key mode of enzyme inhibition by DTG. We propose that DTG, acting as a Zn^{2+} -chelator, can significantly inhibit growth of *A. fumigatus* completely deficient in essential oxidation or thiomethylation activities. Unbiased LFQ proteomics reveals that Zn^{2+} can significantly modify the nature and extent of protein abundance alterations caused by *A. fumigatus* ΔgliT exposure to gliotoxin. This important revelation confirms *in vivo* interaction between both molecular species. Moreover, additional LFQ proteomic data reveal that *in vitro*, DTG can cause specific protein aggregation, manifested by heat instability, possibly due to structural alteration to known Zn^{2+} -dependent enzymes. These unexpected observations open a new front in our exploration of the metallo-metabolome in fungi, and possibly other species.

High resolution, negative mode MS revealed that DTG complexes Zn^{2+} and exhibits a monoisotopic peak with m/z 424.93749, which equates to a single $\text{Zn}^{2+}[\text{DTG}]$ complex detected as a Cl^- adduct $[(\text{DTG} + {}^{64}\text{Zn})-2\text{H} + \text{Cl}]^-$. Previous work by Woodcock *et al.* proposed the existence of a similar adduct (m/z 427), following NaBH_4 -mediated reduction.²⁴ Since no spectra were provided, it is not possible to ascertain the origin of the different observed m/z values, although it seems likely that Woodcock *et al.* reported the average m/z for the compound or the m/z of the base peak $[(\text{DTG} + {}^{66}\text{Zn})-2\text{H} + \text{Cl}]^-$, rather than the monoisotopic peak.²⁴ In addition, we have found that DTG efficiently chelates Zn^{2+} from $\text{Zn}(\text{PAR})_2$ (60 μM), in a dose-dependent manner from 60 to 300 μM DTG. Given that Kocyla *et al.* have proposed an effective pK_a of 12.15 at pH 7.4 for $\text{Zn}(\text{PAR})_2$, it is clear that the affinity of DTG for Zn^{2+} must equate to, or exceed, this value as Zn^{2+} is removed from the $\text{Zn}(\text{PAR})_2$ complex when equimolar amounts of DTG are added to it.⁴⁴ However, it is not ideal to compare these complexes directly due to differences in stoichiometry. Chan *et al.* also deployed a PAR-based assay system, which involved chelation of Zn^{2+} from $\text{Zn}(\text{PAR})_2$, and subsequent formation of stable complexes to reveal that Zn^{2+} is chelated by dithiol holomycin (Fig. 1; termed red-holomycin in Chan *et al.*) with high affinity.³⁰ Davis *et al.* previously revealed and characterised alkylation of DTG using 5'-iodoacetamidofluorescein.⁴⁵ In the present study, we observed that IAA-mediated alkylation of DTG was inhibited by Zn^{2+} , which further underpins our proposal that a $\text{Zn}[\text{DTG}]$ complex is formed *via* thiolate coordination and is stable under *in vitro* conditions used.

DTG acts as a potent inhibitor of the Zn^{2+} -dependent enzyme, AP. Previous studies have reported the inhibitory effects of gliotoxin on mammalian Zn^{2+} -dependent enzymes, without attributing this

activity to zinc chelation.^{16,17} Vigushin *et al.* studied the inhibition of Zn^{2+} -dependent farnesyltransferase (FTase) and geranyltransferase (GGTase) I by gliotoxin, proposing thiol modification of these enzymes as a possible mechanism of action. Importantly, the authors noted that these assays required the reductant DTT, which aligns with our observations of the inhibition of Zn^{2+} -dependent metalloenzymes (*i.e.*, AP) by DTG rather than gliotoxin. Our data also provides an alternative explanation for previous observations which suggested that reducing agents enhanced the inhibitory activity of gliotoxin against a Zn^{2+} -dependent equine ADH.¹⁶ Although these authors posited a redox explanation, it is equally plausible that Zn^{2+} chelation by DTG effected equine ADH inhibition. This accords with our observations that prior incubation of DTG with Zn^{2+} prevents inactivation of AP, and also that DTG-associated AP inhibition can be rescued by subsequent addition of Zn^{2+} (Fig. 3 and Fig. S6, ESI†).

Relevantly, it has been shown that ETPs, in particular gliotoxin, block the interaction between Hypoxia Inducible Factor- α (HIF- α) and the transcriptional coactivator p300 by a Zn^{2+} ejection mechanism.¹⁸ Moreover, these authors noted the antiproliferative effects of ETPs, and provide significant insight into their mechanism of action in animal cells. Cook *et al.* reference the Zn^{2+} -dependency of many gliotoxin-sensitive enzymes and the Zn^{2+} requirement of GliZ, the transcription factor essential for gliotoxin biosynthesis.^{1,18} However, their proposed mechanism of action of Zn^{2+} ejection from p300 by gliotoxin does not take into account the presence of DTT in assay buffers.¹⁸ Thus, consequent to our observations with AP and those of Cook *et al.*, we now speculate that it is DTG, formed due to the presence of equivalent amounts of DTT, and not gliotoxin *per se*, which causes Zn^{2+} ejection from p300. Relevantly, it has recently been elegantly demonstrated that dithiol holomycin (Fig. 1) can effect Zn^{2+} chelation and cause inhibition of a metallo- β -lactamase.³⁰ Our demonstration of DTG-mediated inhibition of AP suggests that the Zn^{2+} chelation potential of dithiolopyrrolones, like holomycin, extends to ETPs.

Our deployment of *A. fumigatus* mutants deficient in gliotoxin self-protection (ΔgliT) and self-protection/negative regulation of gliotoxin biosynthesis in combination ($\Delta\text{gliT}::\Delta\text{gtmA}$) reveal a hitherto unknown systems interaction between Zn^{2+} and gliotoxin biochemistry. We have observed the *in vitro* inhibition of GtmA-mediated BmGT formation by Zn^{2+} . This mode of inhibition appears to result from DTG chelation of Zn^{2+} , and its subsequent unavailability as a substrate to GtmA, as opposed to direct enzyme inhibition. Interestingly, this observation is in accordance with the effect of Zn^{2+} (1 and 2 mM) exposure towards *A. fumigatus* ΔgliT , whereby combinatorial gliotoxin/ Zn^{2+} exposure significantly augments growth inhibition. In effect, we postulate that elevated levels of Zn^{2+} may augment intracellular $\text{Zn}(\text{DTG})$ complex formation, resulting in non-availability to GtmA, which actually significantly increases GtmA abundance (Fig. 5A). Thus, we speculate that Zn^{2+} -mediated disruption of GtmA functionality in *A. fumigatus* ΔgliT partially creates an inability to dissipate DTG, though not as absolute as pertains in *A. fumigatus* $\Delta\text{gliT}::\Delta\text{gtmA}$. Indeed, *A. fumigatus* $\Delta\text{gliT}::\Delta\text{gtmA}$ presents an ideal system to explore the functionality of Zn^{2+} -dependent systems in fungi, since the



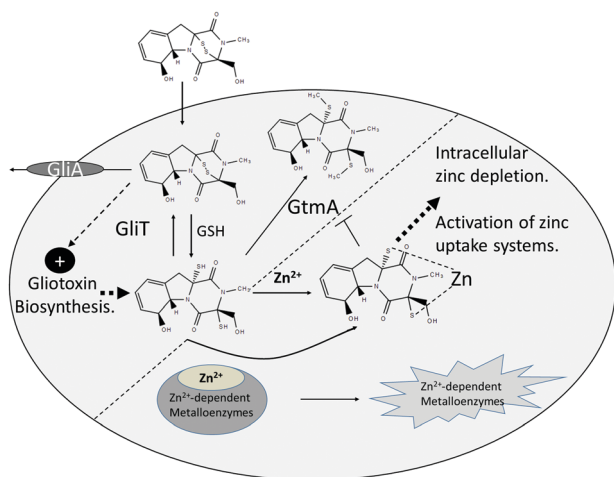


Fig. 6 Overview of the proposed mechanism and consequences of Zn^{2+} chelation by intracellular DTG in *A. fumigatus*. DTG is produced consequent to gliotoxin uptake, via GSH-mediated chemical reduction, or *de novo* gliotoxin biosynthesis. Under normal conditions, two enzyme systems, namely GliT-mediated oxidation and GtmA-mediated thiomethylation effect dismutation of DTG to prevent interference with intracellular zinc homeostasis. In the absence of both enzymes, elevated intracellular DTG can either chelate free Zn^{2+} or chelate it from intracellular Zn^{2+} -dependent metalloenzymes, causing extreme growth inhibition. Additionally, $\text{Zn}(\text{DTG})$ cannot be converted to BmGT via GtmA. Either way, disruption of intracellular zinc homeostasis occurs which leads to activation of zinc uptake systems, potentially via ZafA induction of ZrfA-C expression.

organism lacks both enzymes, GliT and GtmA, which contribute to dissipation of intracellular DTG (Fig. 6), ultimately via either gliotoxin or BmGT efflux.¹⁵ The significant, though incomplete, Zn^{2+} -mediated reversal of *A. fumigatus* $\Delta\text{gliT}::\Delta\text{gtmA}$ sensitivity to exogenous gliotoxin exposure implicates either chelation of free Zn^{2+} or chelation of Zn^{2+} from cellular metalloenzymes, by DTG as key inhibitory mechanisms (Fig. 6). To our knowledge, this is the first report of an *in vivo* interaction between gliotoxin biosynthesis, dysregulated DTG presence and growth inhibition due to potential interference with Zn^{2+} -associated growth systems. Moreover, it contributes to explaining the cryptic observation of Dolan *et al.* that *A. fumigatus* $\Delta\text{gliT}::\Delta\text{gtmA}$ is the most gliotoxin-sensitive mutant observed to date,¹⁵ and also why there are two distinct enzymatic activities which can prevent intracellular DTG accumulation. Overall, these data indicate the inhibitory potential of this endogenous, and potent, Zn^{2+} chelator in *A. fumigatus* in particular, and possibly microorganisms in general. Indeed, gliotoxin significantly inhibits growth of a range of fungi,^{12,46} and previously work has also indicated its potent anti-bacterial activity.⁴⁷

It is clear that interference with intracellular DTG levels, via gliotoxin exposure to *A. fumigatus* ΔgliT impacts on the fungal proteome, which in turn can be modulated by Zn^{2+} presence. Indeed, it has been estimated that up to 6% (600/10 000) of the *A. fumigatus* proteome comprises Zn^{2+} -binding proteins; interestingly, this includes a prediction of 300 Zn^{2+} finger transcription factors.⁴⁸ Relevantly, co-addition of gliotoxin and Zn^{2+} induced key alterations to abundance of proteins involved in secondary metabolism. Proteins from the gliotoxin biosynthetic cluster, GliM and GliH, were uniquely detected in

mycelia exposed to gliotoxin, indicating that combinatorial exposure with Zn^{2+} prevents activation of gliotoxin cluster expression. While GliM and GliH are induced in response to gliotoxin, these proteins are not detected following BmGT exposure.⁹ This may implicate Zn^{2+} chelation in the activation of the gliotoxin transcription factor GliZ and the induction of cluster expression. O'Keeffe *et al.* noted gliotoxin exposure suppresses fumagillin cluster expression in *A. fumigatus* ΔgliT .¹⁴ This result was reflected in the current study, however co-exposure to gliotoxin and Zn^{2+} reversed this effect, leading to unique detection of fumagillin biosynthetic proteins. As with gliotoxin, the fumagillin cluster is also regulated by a $(\text{Zn}^{2+})_2\text{Cys}_6$ transcription factor (FapR/FumR),^{49,50} possibly implicating Zn^{2+} chelation in cluster repression, since exogenous Zn^{2+} blocks gliotoxin-associated repression. These proteomic observations are supported by the switch from gliotoxin to fumagillin production in *A. fumigatus* upon Zn^{2+} supplementation (Fig. S10, ESI[†]).

Incubation of *A. fumigatus* protein lysates with DTG prior to heat treatment resulted in increased protein aggregation, compared to the solvent control. Oxidoreductases, metal-binding proteins and zinc-binding proteins were significantly enriched amongst these DTG-affected proteins ($p < 0.05$). DTG-induced aggregation of zinc-binding proteins including two alcohol dehydrogenases, AlcC and AFUA_1G04620, and the farnesyltransferase (AFUA_4G10330) was observed. This is in line with observed inhibition of mammalian homologs of these proteins by gliotoxin in reducing conditions.^{16,17} AlcC was also observed to increase in abundance *in vivo* when *A. fumigatus* ΔgliT was treated with a combination of gliotoxin and Zn^{2+} compared to gliotoxin alone (Table S1, ESI[†]), possibly to compensate for loss of activity. AlcC has been identified as the primary hypoxia-responsive ADH in *A. fumigatus*, with a potential role in pathogenesis,⁵¹ while farnesyltransferase has a role in signalling and also contributes to disease.⁵² Further investigation could elucidate the effect of DTG on the functionality of these proteins in *A. fumigatus*. Pre-incubation of DTG with excess Zn^{2+} abrogated this effect, most likely through formation of $\text{Zn}(\text{DTG})$ complexes prior to addition to protein lysates, leading to reduced levels of protein aggregation. A number of metalloproteases (AFUA_6G09190, AFUA_4G07910, AFUA_1G14920 and MepB) were also observed to undergo increased aggregation in response to DTG, while this was prevented in the presence of Zn^{2+} . These proteases contribute to protein modification and degradation, and so alteration of these processes by DTG has the potential to disrupt protein turnover. Interestingly, gliotoxin has previously been implicated in inhibition of proteolytic activity of human and toxoplasma proteasomes.^{53,54} The cobalamin-independent methionine synthase Meth/D showed a similar response to DTG treatment, with Zn^{2+} co-addition blocking aggregation. Meth/D contains a zinc-binding site, required for binding and activation of its substrate homocysteine.⁵⁵ DTG-mediated aggregation of Meth/D would interrupt an integral part of primary metabolism and potentially affect pathogenesis.⁵⁶ Interestingly, while *meth/D* showed no response to gliotoxin in *A. fumigatus* wild-type, expression was significantly induced in *A. fumigatus* ΔgliT in response to gliotoxin.¹⁴ Persistence of intracellular DTG, in the



absence of GliT-mediated oxidation, results in disruption of the methionine cycle, with SAM depletion caused by dysregulation of gliotoxin methylation.⁸ Added to the extensive SAM consumption, DTG-associated destabilisation of methionine synthase through Zn²⁺-chelation could place an additional strain on the methionine cycle in *A. fumigatus* Δ gliT. While further studies are required to confirm if these proteins are directly affected by DTG *in vivo*, these results present strong targets for future investigations to elucidate the systemic effect of DTG on *A. fumigatus*. Of course, Zn²⁺ chelation is likely not the only mechanism by which DTG exerts its effects on the cell, with previous studies illustrating its potential for thiol modification and redox reactions.^{57,58} This methodology also provides an unbiased discovery-based mechanism allowing for the identification of putative targets of DTG in other complex systems.

Interestingly, Müller *et al.* have shown that allicin (diallyl thiosulphinate) can cause thiol stress and severe growth inhibition in bacteria.⁵⁹ Specifically, Muller *et al.* revealed that allicin induced protein aggregation, likely due to *S*-allylmercapto protein modification, in crude *Escherichia coli* cell lysates in a concentration-dependent manner. This is in accordance with our observations of DTG-induced protein aggregation in *A. fumigatus* protein lysates, although fungal protein destabilisation possibly involves Zn²⁺ chelation mechanism, as opposed to protein modification. Future work will clarify the relative contribution of either mechanism.

As can be seen in Fig. S8 (ESI[†]), gliotoxin addition to *A. fumigatus* results in uptake, followed by conversion to intracellular DTG and induction/augmentation of gliotoxin biosynthesis, as previously reported in Owens *et al.* and Dolan *et al.*^{8,15} Based on our new observations, we now extend this model and provide a mechanistic link between the intracellular presence of DTG and (i) Zn²⁺ depletion leading to increased ZrfB abundance, as well as (ii) potential Zn²⁺ chelation and destabilisation of metallo-enzymes. Interestingly, the membrane-permeable zinc chelator, TPEN, which has been used *in vivo*⁶⁰ and in *A. fumigatus* studies,⁶¹ demonstrated lower AP inhibition than DTG (Fig. 3). The dissociation constant (K_d) of Zn(TPEN) has been reported as 6.4×10^{-16} M (pK_d 15.2) at pH 7.4, with the same 1:1 stoichiometry as the Zn(DTG) complex.^{62,63} Future studies will quantify the affinity of DTG for Zn²⁺ however, considering DTG caused significantly greater AP inhibition than TPEN, it is reasonable to conclude that DTG is a better Zn²⁺ chelator than TPEN under the conditions tested. TPEN has been shown to act co-operatively with the antifungal drug caspofungin to significantly improve survival in a mouse model system of Invasive Pulmonary Aspergillosis compared to either caspofungin or TPEN administration alone.⁶⁴ This exciting development is important because exposure to combinations of antifungal drugs, acting in synergy, may address both the development of pathogen resistance and toxicity of high therapeutic levels of either drug alone to the recipient. Although TPEN administration may not have any immediate harmful effects in animals, its safety profile following co-administration with antifungal drugs is unknown. Our observation of DTG as an intracellular Zn²⁺ chelator, ideally positions it as a potential endogenous anti-fungal, especially if strategies to interfere with its enzymatic elimination are elucidated in future research.

Conclusions

Overall, new *in vivo* and *in vitro* interactions between Zn²⁺ and DTG, with multiple biological consequences, are revealed. *A. fumigatus* is a pathogen for which limited therapeutic options exist. Although much recent work has greatly increased the understanding of this and other fungal species, investigation of cryptic interaction between Zn²⁺ and BGC-encoded metabolite functionality needs urgent study. Any new systems identified could not only represent antifungal drug targets, but also inform on the exploitation of BGC-encoded, dithiol-containing, metabolites to restrict Zn²⁺ availability in many microbial species.

Conflicts of interest

There are no conflicts to declare.

Acknowledgements

AAS was funded by a Government of Ireland Postdoctoral Fellowship from the Irish Research Council (GOIPD/2015/516). SFD was funded by a SPUR studentship from Maynooth University. Mass spectrometry facilities were funded by Science Foundation Ireland (12/RI/2346 (3)) and the Irish Higher Education Authority.

References

- 1 J. W. Bok, D. Chung, S. A. Balajee, K. A. Marr, D. Andes, K. F. Nielsen, J. C. Frisvad, K. A. Kirby and N. P. Keller, *Infect. Immun.*, 2006, **74**, 6761–6768.
- 2 R. A. Owens, G. O'Keeffe, K. A. O'Hanlon, L. Gallagher and S. Doyle, in *Human Pathogenic Fungi: Molecular Biology and Pathogenic Mechanisms*, ed. D. J. Sullivan and G. P. Moran, Caister Academic Press, 2014, pp. 163–194.
- 3 B. Li, W. J. Wever, C. T. Walsh and A. A. Bowers, *Nat. Prod. Rep.*, 2014, **31**, 905–923.
- 4 S. K. Dolan, G. O'Keeffe, G. W. Jones and S. Doyle, *Trends Microbiol.*, 2015, **23**, 419–428.
- 5 D. H. Scharf, N. Remme, T. Heinekamp, P. Hortschansky, A. A. Brakhage and C. Hertweck, *J. Am. Chem. Soc.*, 2010, **132**, 10136–10141.
- 6 B. Li and C. T. Walsh, *Biochemistry*, 2011, **50**, 4615–4622.
- 7 M. Schrettl, S. Carberry, K. Kavanagh, H. Haas, G. W. Jones, J. O'Brien, A. Nolan, J. Stephens, O. Fenelon and S. Doyle, *PLoS Pathog.*, 2010, **6**, e1000952.
- 8 R. A. Owens, G. O'Keeffe, E. B. Smith, S. K. Dolan, S. Hammel, K. J. Sheridan, D. A. Fitzpatrick, T. M. Keane, G. W. Jones and S. Doyle, *Eukaryotic Cell*, 2015, **14**, EC.00055.
- 9 S. K. Dolan, R. A. Owens, G. O'Keeffe, S. Hammel, D. A. Fitzpatrick, G. W. Jones and S. Doyle, *Chem. Biol.*, 2014, **21**, 999–1012.
- 10 B. Li, R. R. Forseth, A. A. Bowers, F. C. Schroeder and C. T. Walsh, *ChemBioChem*, 2012, 1–7.
- 11 P. H. Bernardo, N. Brasch, C. L. L. Chai and P. Waring, *J. Biol. Chem.*, 2003, **278**, 46549–46555.



- 12 S. Carberry, E. Molloy, S. Hammel, G. O'Keeffe, G. W. Jones, K. Kavanagh and S. Doyle, *Fungal Genet. Biol.*, 2012, **49**, 302–312.
- 13 R. A. Cramer, M. P. Gamcsik, R. M. Brooking, L. K. Najvar, W. R. Kirkpatrick, T. F. Patterson, C. J. Balibar, J. R. Graybill, J. R. Perfect, S. N. Abraham and W. J. Steinbach, *Eukaryotic Cell*, 2006, **5**, 972–980.
- 14 G. O'Keeffe, S. Hammel, R. A. Owens, T. M. Keane, D. A. Fitzpatrick, G. W. Jones and S. Doyle, *BMC Genomics*, 2014, **15**, 894.
- 15 S. K. Dolan, T. Bock, V. Hering, R. A. Owens, G. W. Jones, W. Blankenfeldt and S. Doyle, *Open Biol.*, 2017, **7**, 160292.
- 16 P. Waring, A. Sjaarda and Q. H. Lin, *Biochem. Pharmacol.*, 1995, **49**, 1195–1201.
- 17 D. M. Vigushin, N. Mirsaidi, G. Brooke, C. Sun, P. Pace, L. Inman, C. J. Moody and R. C. Coombes, *Med. Oncol.*, 2004, **21**, 21–30.
- 18 K. M. Cook, S. T. Hilton, J. Mecnovic, W. B. Motherwell, W. D. Figg and C. J. Schofield, *J. Biol. Chem.*, 2009, **284**, 26831–26838.
- 19 K. M. Reece, E. D. Richardson, K. M. Cook, T. J. Campbell, S. T. Pisle, A. J. Holly, D. J. Venzon, D. J. Liewehr, C. H. Chau, D. K. Price and W. D. Figg, *Mol. Cancer*, 2014, **13**, 91.
- 20 L. Lauinger, J. Li, A. Shostak, I. A. Cemel, N. Ha, Y. Zhang, P. E. Merkl, S. Obermeyer, N. Stankovic-Valentin, T. Schafmeier, W. J. Wever, A. A. Bowers, K. P. Carter, A. E. Palmer, H. Tschochner, F. Melchior, R. J. Deshaies, M. Brunner and A. Diernfellner, *Nat. Chem. Biol.*, 2017, **13**, 709–714.
- 21 A. Abad, J. V. Fernández-Molina, J. Bikandi, A. Ramírez, J. Margareto, J. Sendino, F. Luis Hernando, J. Pontón, J. Garaizar and A. Rementeria, *Rev. Iberoam. Micol.*, 2010, **27**, 155–182.
- 22 C. Coméra, K. André, J. Laffitte, X. Collet, P. Galtier and I. Maridonnew-Parini, *Microbes Infect.*, 2007, **9**, 47–54.
- 23 J. J. Bennison, R. M. Nottingham, E. L. Key and J. J. Parkins, *N. Z. Vet. J.*, 2010, **58**, 201–206.
- 24 J. C. Woodcock, W. Henderson and C. O. Miles, *J. Inorg. Biochem.*, 2001, **85**, 187–199.
- 25 M. A. Moreno, O. Ibrahim-Granet, R. Vicentefranqueira, J. Amich, P. Ave, F. Leal, J.-P. Latge and J. A. Calera, *Mol. Microbiol.*, 2007, **64**, 1182–1197.
- 26 J. Amich, R. Vicentefranqueira, E. Mellado, A. Ruiz-Carmuega, F. Leal and J. A. Calera, *Cell. Microbiol.*, 2014, **16**, 548–564.
- 27 R. Vicentefranqueira, J. Amich, P. Laskaris, O. Ibrahim-Granet, J. P. Latge, H. Toledo, F. Leal and J. A. Calera, *Front. Microbiol.*, 2015, **6**, 160.
- 28 S. Yasmin, B. Abt, M. Schrettl, T. A. A. Moussa, E. R. Werner and H. Haas, *Fungal Genet. Biol.*, 2009, **46**, 707–713.
- 29 S. Doyle, G. W. Jones and S. K. Dolan, *Fungal Biol.*, 2018, **122**, 214–221.
- 30 A. N. Chan, A. L. Shiver, W. J. Wever, S. Z. A. Razvi, M. F. Traxler and B. Li, *Proc. Natl. Acad. Sci. U. S. A.*, 2017, **114**, 2717–2722.
- 31 E. B. Smith, S. K. Dolan, D. A. Fitzpatrick, S. Doyle and G. W. Jones, *Microb. Cell*, 2016, **3**, 120–125.
- 32 N. M. Moloney, R. A. Owens, P. Meleady, M. Henry, S. K. Dolan, E. Mulvihill, M. Clynes and S. Doyle, *J. Proteomics*, 2016, **136**, 99–111.
- 33 J. Cox, M. Y. Hein, C. A. Lubner, I. Paron, N. Nagaraj and M. Mann, *Mol. Cell. Proteomics*, 2014, **13**, 2513–2526.
- 34 S. Tyanova, T. Temu, P. Sinitcyn, A. Carlson, M. Y. Hein, T. Geiger, M. Mann and J. Cox, *Nat. Methods*, 2016, **13**, 731–740.
- 35 S. Priebe, C. Kreisel, F. Horn, R. Guthke and J. Linde, *Bioinformatics*, 2015, **31**, 445–446.
- 36 A. Shevchenko, H. Tomas, J. Havlis, J. V. Olsen and M. Mann, *Nat. Protoc.*, 2007, **1**, 2856–2860.
- 37 L. Manzanares-Miralles, Ö. Sarikaya-Bayram, E. B. Smith, S. K. Dolan, Ö. Bayram, G. W. Jones and S. Doyle, *J. Proteomics*, 2016, **131**, 149–162.
- 38 L. Gallagher, R. A. Owens, G. O'Keeffe, S. K. Dolan, M. Schrettl, K. Kavanagh, G. Jones and S. Doyle, *Eukaryotic Cell*, 2012, **11**, 1226–1238.
- 39 J. Amich, R. Vicentefranqueira, F. Leal and J. A. Calera, *Eukaryotic Cell*, 2010, **9**, 424–437.
- 40 K.-S. Shin, N.-J. Kwon and J.-H. Yu, *Curr. Genet.*, 2009, **55**, 631–641.
- 41 K. A. O'Hanlon, T. Cairns, D. Stack, M. Schrettl, E. M. Bignell, K. Kavanagh, S. M. Miggin, G. O'Keeffe, T. O. Larsen and S. Doyle, *Infect. Immun.*, 2011, **79**, 3978–3992.
- 42 M. F. Mabanglo, M. A. Hast, N. B. Lubock, H. W. Hellinga and L. S. Beese, *Protein Sci.*, 2014, **23**, 289–301.
- 43 H.-W. Park, S. R. Boduluri, J. F. Moomaw, P. J. Casey and L. S. Beese, *Science*, 1997, **275**, 1800–1805.
- 44 A. Kocyla, A. Pomorski and A. Krezel, *J. Inorg. Biochem.*, 2015, **152**, 82–92.
- 45 C. Davis, N. Gordon, S. Murphy, I. Singh, K. Kavanagh, S. Carberry and S. Doyle, *Anal. Bioanal. Chem.*, 2011, **401**, 2519–2529.
- 46 J. J. Coleman, S. Ghosh, I. Okoli and E. Mylonakis, *PLoS One*, 2011, **6**, e25321.
- 47 W.-L. Liang, X. Le, H.-J. Li, X.-L. Yang, J.-X. Chen, J. Xu, H.-L. Liu, L.-Y. Wang, K.-T. Wang, K.-C. Hu, D.-P. Yang and W.-J. Lan, *Mar. Drugs*, 2014, **12**, 5657–5676.
- 48 C. C. Staats, L. Kmetzsch, A. Schrank and M. H. Vainstein, *Front. Cell. Infect. Microbiol.*, 2013, **3**, 65.
- 49 P. Wiemann, C. Guo, J. M. Palmer, R. Sekonyela and C. C. Wang, *Proc. Natl. Acad. Sci. U. S. A.*, 2013, **110**, 17065–17070.
- 50 S. Dhingra, A. L. Lind, H. C. Lin, Y. Tang, A. Rokas and A. M. Calvo, *PLoS One*, 2013, **8**, 1–16.
- 51 N. Grahl, S. Puttikamonkul, J. M. Macdonald, M. P. Gamcsik, L. Y. Ngo, T. M. Hohl and R. A. Cramer, *PLoS Pathog.*, 2011, **7**, e1002145.
- 52 T. S. Norton, Q. Al Abdallah, A. M. Hill, R. V. Lovingood and J. R. Fortwendel, *Virulence*, 2017, **8**, 1401–1416.
- 53 M. Kroll, F. Arenzana-Seisdedos, F. Bachelier, D. Thomas, B. Friguet and M. Conconi, *Chem. Biol.*, 1999, **6**, 689–698.
- 54 A. Paugam, C. Creuzet, J. Dupouy-Camet and P. Roisin, *Parasitol. Res.*, 2002, **88**, 785–787.
- 55 R. W. Wheatley, K. K. S. Ng and M. Kapoor, *Arch. Biochem. Biophys.*, 2016, **590**, 125–137.
- 56 J. Amich, M. Dümig, G. O'Keeffe, J. Binder, S. Doyle, A. Beilhack and S. Krappmann, *Infect. Immun.*, 2016, IAL01124.



- 57 R. D. Eichner, P. Waring, A. M. Geue, A. W. Braithwaite and A. Mullbacher, *J. Biol. Chem.*, 1988, **263**, 3772–3777.
- 58 A. M. Hurne, C. L. L. Chai and P. Waring, *J. Biol. Chem.*, 2000, **275**, 25202–25206.
- 59 A. Müller, J. Eller, F. Albrecht, P. Prochnow, K. Kuhlmann, J. E. Bandow, A. J. Slusarenko and L. I. O. Leichert, *J. Biol. Chem.*, 2016, **291**, 11477–11490.
- 60 E. Cho, J.-J. Hwang, S.-H. Han, S. J. Chung, J.-Y. Koh and J.-Y. Lee, *Neurotoxic. Res.*, 2010, **17**, 156–166.
- 61 S. J. Luloff, B. L. Hahn and P. G. Sohnle, *J. Lab. Clin. Med.*, 2004, **144**, 208–214.
- 62 A. Krężel and W. Maret, *Arch. Biochem. Biophys.*, 2016, **611**, 3–19.
- 63 A. E. Martell and R. M. Smith, *Critical Stability Constants*, Plenum Press, New York, 1974.
- 64 P. Laskaris, A. Atrouni, J. A. Calera, C. d'Enfert, H. Munier-Lehmann, J.-M. Cavaillon, J.-P. Latge and O. Ibrahim-Granet, *Antimicrob. Agents Chemother.*, 2016, **60**, 5631–5639.

